



Supplement of

A seismic analysis of subglacial lake D2 (Subglacial Lake Cheongsuk) beneath David Glacier, Antarctica

Hyeontae Ju et al.

Correspondence to: Seung-Goo Kang (ksg9322@kopri.re.kr)

The copyright of individual parts of the supplement might differ from the article licence.

9 S1. Seismic data acquisition

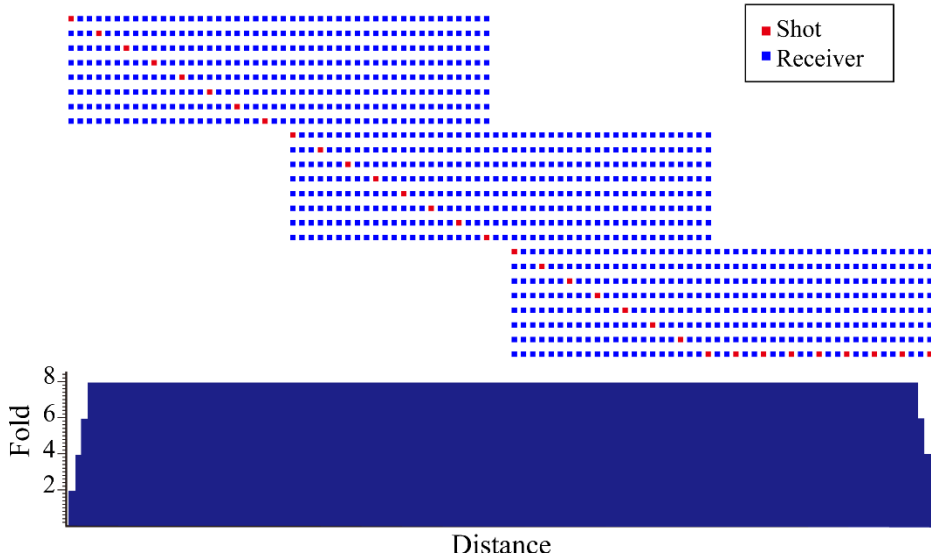
10

11 **Table S1: Seismic survey work schedules**

Date (dd/mm/yy)	Job	Work day (day)
01/12/21	GPR survey	1
04/12/21 – 05/12/21	Marked shot position	2
06/12/21 – 28/12/21	Hot water drilling (25 m) and explosive installation (4 lines, total 144 points)	14
12/12/21 – 02/01/22	Seismic survey (4 lines)	11

12

13



14

15 **Figure S1: In the seismic survey layout, only the odd-numbered receivers are displayed, that is, one receiver marked every two**
16 **channels.**

17

18 S2. Seismic data processed parameters and results

19 This study utilized the Omega geophysical data processing platform (SLB) for seismic data processing. Among the various
20 processing steps, we provide below the key parameters applied during procedures that directly influence the ice–bedrock
21 interface signal, such as noise attenuation.

22

23 1. Anomalous amplitude attenuation (AAA) for the 1st round

24 AAA is a frequency-domain filtering technique designed to suppress spatially coherent anomalous amplitudes such as swell
25 noise and rig noise, by comparing amplitude spectra across traces and attenuating outliers based on spatial median statistics.
26 The method identifies frequency bands with anomalous energy by comparing each trace's amplitude spectrum within a spatial
27 window to the median of its neighboring traces. Detected anomalies are either scaled or replaced using interpolated values
28 from adjacent traces, preserving relative amplitude relationships. Key parameters include TIME, which defines the temporal
29 window of threshold application; THRESHOLD FACTOR, which sets the amplitude level considered anomalous; and
30 SPATIAL MEDIAN WIDTH, which specifies the number of adjacent traces used for median computation. Proper tuning of
31 these parameters is essential to avoid signal distortion while effectively attenuating coherent noise. AAA is particularly useful
32 in prestack data conditioning as it enhances seismic data quality without compromising true subsurface reflections (SLB,
33 2025a).

34

- SPATIAL MEDIAN WIDTH: 21 traces
- Threshold factor tables:

TIME	THRESHOLD FACTOR
0	15
1000	10
3000	7
4000	6

36

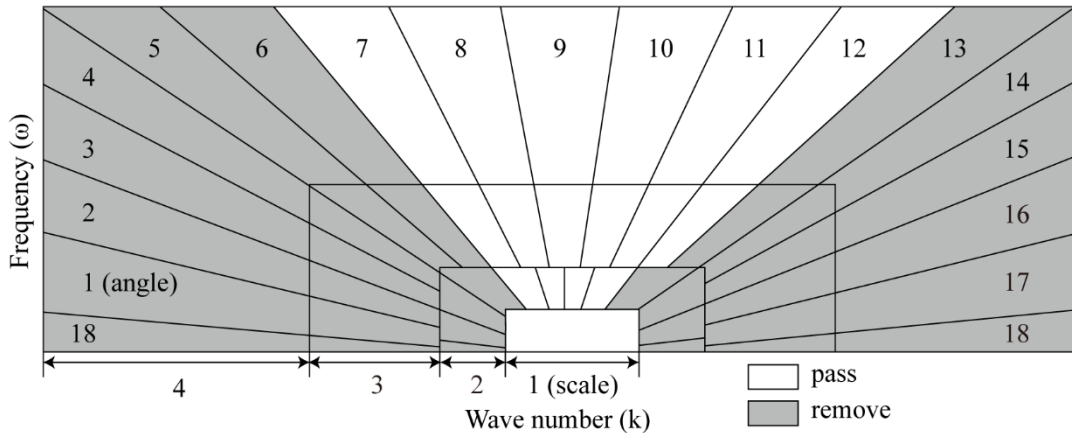
37 2. Curvelet transform-based filter for 1st round

38 Curvelet Transform is a multi-scale, multi-directional decomposition technique that provides a sparse representation of seismic
39 data by capturing curved wavefronts more efficiently than conventional fourier or wavelet transforms. An important aspect of
40 the Curvelet Transform implementation involves user-defined control over the scale and angle bounds that determine which
41 components of the data will be transformed. The LOWER BOUND OF SCALE and HIGHER BOUND OF SCALE specify
42 the range of spatial frequencies (scales) to be included in the transform. Lower scales correspond to coarse, low-frequency
43 components, while higher scales capture fine, high-frequency structural details. The LOWER BOUND OF ANGLE and

44 HIGHER BOUND OF ANGLE define the directional sectors (angles) within each scale to be analyzed. This allows selective
 45 enhancement or suppression of events based on their dip or propagation direction (SLB, 2025b). Figure S2 illustrates how the
 46 f-k domain is partitioned into curvelet panels by scale and angle. Adjusting these bounds allows for targeted signal processing,
 47 such as isolating curved events or attenuating directionally coherent noise. These parameters provide valuable flexibility in
 48 customizing the transform for specific seismic applications.

49 ● Panel manager

LOWER BOUND OF THE SCALE	HIGHER BOUND OF THE SCALE	LOWER BOUND OF THE ANGLE	HIGHER BOUND OF THE ANGLE
2	2	1	3
2	2	8	10
3	3	1	6
3	3	13	18
4	4	1	6
4	4	13	18



50

51 **Figure S2: Illustration of the panel manager. In the f-k domain, the hatched area is identified as noise and removed accordingly.**

52

53 3. Surface-consistent deconvolution

54 Surface-Consistent Deconvolution is a technique for generating and applying deconvolution operators that are consistent across
 55 seismic sources, receivers, offset ranges, and CMP locations (SLB, 2025c; Yilmaz, 2001).

56 Key processing parameters used in this workflow include:

57 ● CONSTANT_ACOR_LENGTH = 100: Defines the half-length of the autocorrelation window used in operator
 58 design, balancing spectral resolution and filter stability.

59

60 ● WHITE NOISE PERCENT = 0.01: Adds 1% white noise to stabilize the autocorrelation estimation and prevent
61 over-whitening of the signal.

62 ● PREDICTION DISTANCE = 2.5: Specifies the prediction lag in the predictive filter design; this parameter
63 controls the temporal range of the filter's effect, influencing multiple suppression and resolution.

64

65 4. Anomalous amplitude attenuation (AAA) for the 2nd round

66 ● Spatial median width: 11 traces

67 ● Threshold factor tables:

Time	Threshold factor
0	8
1000	6
3000	4
4000	3

68

69 5. Curvelet transform-based filter for the 1st round: same as 1st round parameter

70

71 6. Frequency-offset coherent noise suppression (Figure S4.c)

72 The frequency-offset (F-X) Coherent Noise Suppression (FXCNS) module is designed to attenuate near-surface shot-
73 generated coherent noise, such as dispersive surface waves and trapped modes, which interfere with primary seismic reflections,
74 particularly in 3D shot or receiver gathers with irregular spatial sampling (Hildebrand, 1982). FXCNS operates in the frequency
75 domain by modeling coherent noise using fan filters and estimating it in a least-squares sense for each trace based on local
76 neighbors within a specified azimuthal sector. The estimated coherent noise is then subtracted from the original signal,
77 preserving true reflection events (SLB, 2025d).

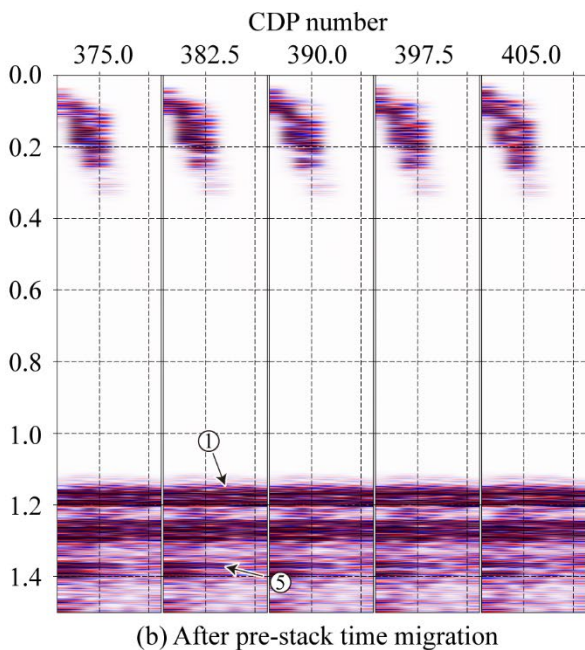
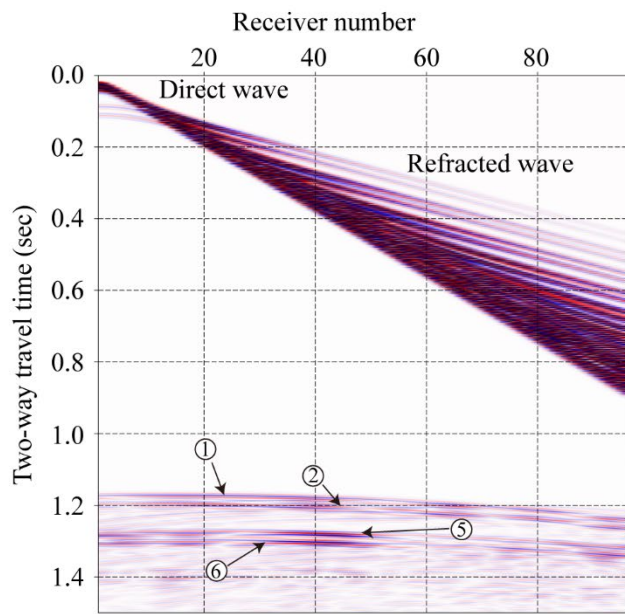
78 ● LOW PASS VELOCITY: 100

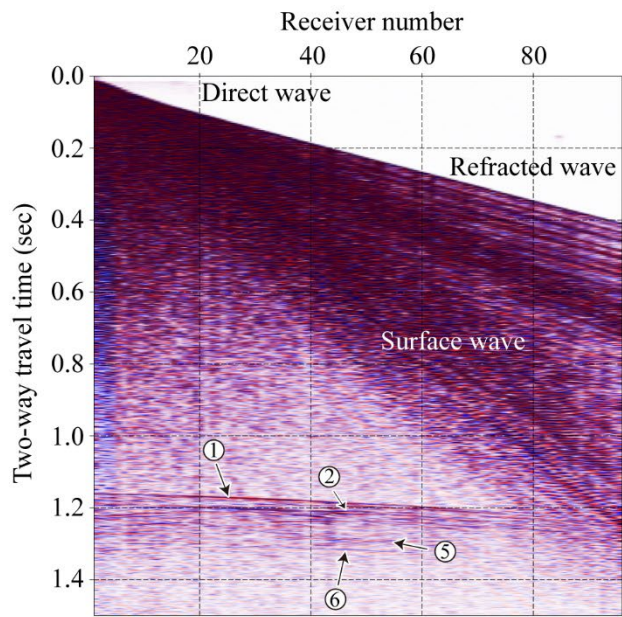
79 ● LOW STOP VELOCITY: 300

80 ● HIGH PASS VELOCITY: 8000

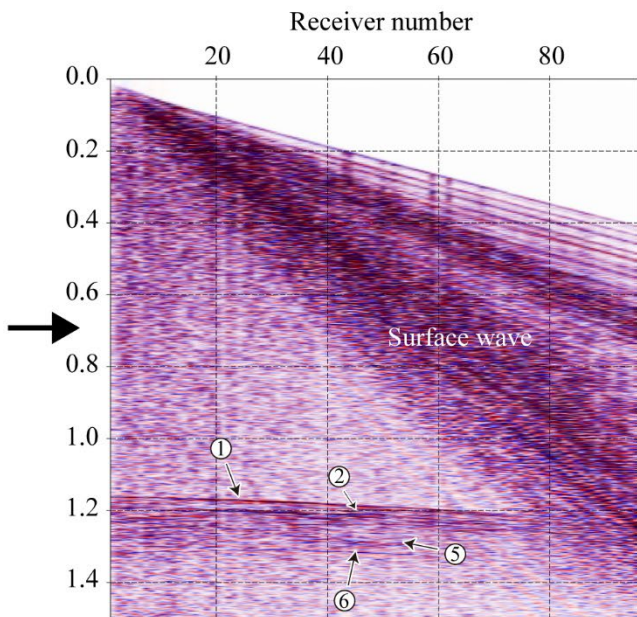
81 ● HIGH STOP VELOCITY: 10000

82

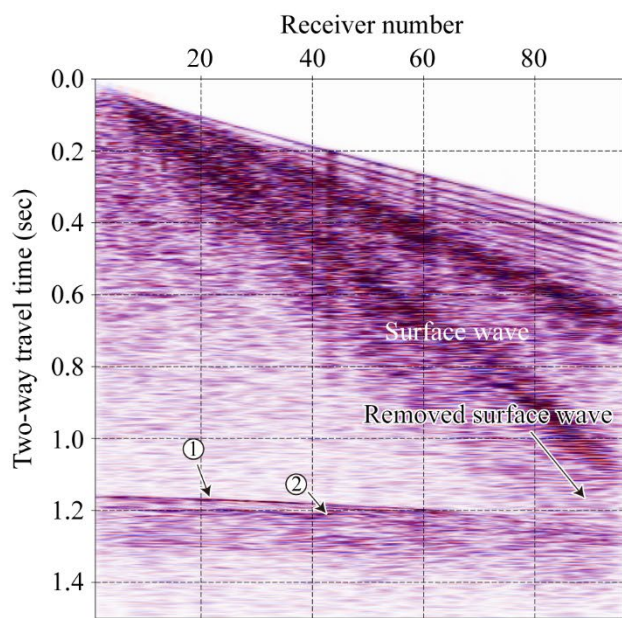




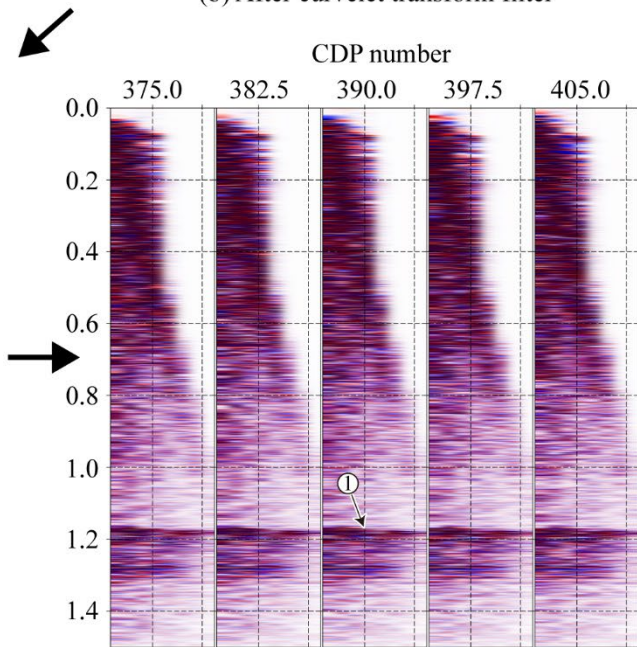
(a) Raw data shot gather of 21YY



(b) After curvelet transform filter



(c) After tau-p linear noise attenuation



(d) After pre-stack time migration

86

87 **Figure S4: Results at each stage of data processing.** (a) Shot gather #1 from 21YY. (b) Removal of high-frequency random noise and
88 coherent linear noise. (c) Application of a frequency-offset coherent noise filter and tau-p linear noise attenuation for surface wave
89 removal. (d) Result after applying pre-stack time migration.

90

91 S3. Seismic data acquisition

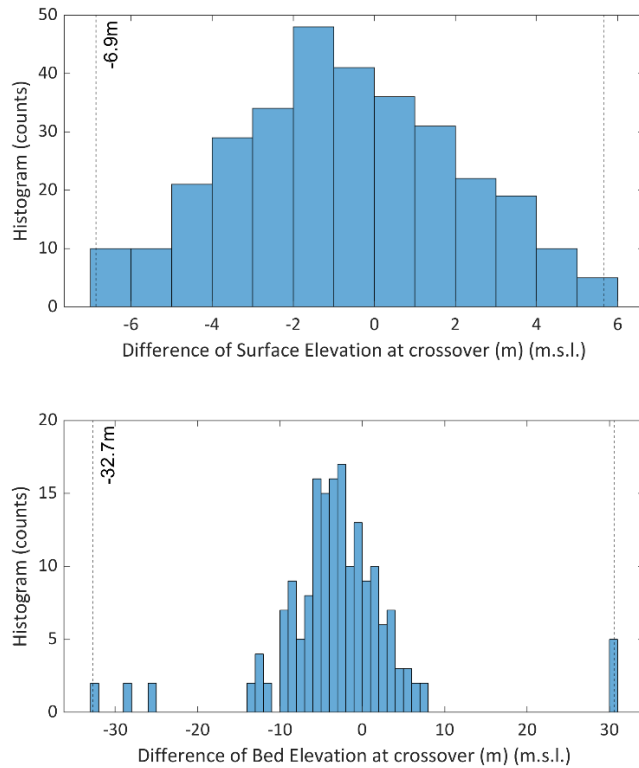
92

93 1. IPR data uncertainty in glacier thickness estimates

94 The vertical uncertainty of the GNSS data was estimated to be 0.98 m. At the 99% confidence level, the uncertainties in surface
95 and bed elevation measurements were calculated as ± 6.9 m and ± 32.7 m, respectively (Figure S5). When incorporating the
96 GNSS vertical uncertainty, the total uncertainties in surface and bed elevations increased slightly to ± 7.0 m and ± 32.7 m,
97 respectively. Consequently, the overall uncertainty of the IPR-derived ice thickness was estimated to be ± 33.4 m.

98
$$U_{IPR} = \sqrt{(\pm 7.0 \text{ m})^2 + (\pm 32.7 \text{ m})^2} = \pm 33.4 \text{ m.}$$
 S3.1

99



100

101 **Figure S5. Measurement uncertainty results of surface and ice bottom elevations from IPR data.**

102

103 2. Seismic data uncertainty in glacier thickness estimates

104 The uncertainty associated with seismic picking arises from the presence of noise and is quantified as picking uncertainty
105 (U_{pick}), which can be estimated using the following equation (Abakunov et al., 2020):

106
$$\sigma_{\text{pick}} = 2 \sqrt{\frac{T^2}{4\pi^2} \frac{1}{SNR}},$$
 S3.2

107 where T is the period of the central frequency and SNR is the signal-to-noise ratio. Based on this formulation, the SNRs of the
108 first arrival and the ice–water interface signals were determined to be 88.8 dB and 10 dB, yielding vertical uncertainties of 0.2
109 m and 2.1 m, respectively.

110
$$U_{pick} = 2.58 \sigma_{pick} = \pm 5.4 \text{ m.} \quad \text{S3.3}$$

111 The total picking uncertainty at the 99% confidence level is 5.4 m. Under glacial temperature conditions of $-2 \pm 2 \text{ }^{\circ}\text{C}$, where
112 the average P-wave velocity in ice is $3800 \pm 5 \text{ m s}^{-1}$ (Kohnen, 1974), the uncertainty associated with the variability in seismic
113 velocity is estimated to be $\pm 5.3 \text{ m}$. Assuming a firn layer thickness of 100 m, the combined measurement uncertainty of the
114 seismic results at the 99% confidence level is calculated to be 7.6 m.

115
$$U_{Seis} = \sqrt{(\pm 5.4 \text{ m})^2 + (\pm 5.3 \text{ m})^2} = \pm 7.6 \text{ m.} \quad \text{S3.4}$$

116

117

119 Abakumov, I., Roeser A., and Shapiro S. A.: Arrival-time picking uncertainty: Theoretical estimations and their
120 application to microseismic data, *Geophysics*, 85, U65–U76, <https://doi.org/10.1190/geo2019-0589.1>, 2020.

121 Hildebrand, S. T.: Two representations of the fan filter, *Geophysics*, 47, 957–959,
122 <https://doi.org/10.1190/1.1441363>, 1982.

123 Kohnen, H.: The temperature dependence of seismic waves in ice, *J. Glaciol.*, 13, 144–147,
124 <https://doi.org/10.3189/s0022143000023467>, 1974.

125 SLB: Omega Geophysical Processing System – Anomalous Amplitude Noise Attenuation
126 (ANOMALOUS_AMP_ATTEN) Module Documentation, Version 27.14, SLB manual, Houston, TX,
127 2025a.

128 SLB: Omega Geophysical Processing System – Curvelet Transform (CURVELET_TRANSFORM) Module
129 Documentation, Version 22.1, SLB manual, Houston, TX, 2025b.

130 SLB: Omega Geophysical Processing System – Surface-Consistent Deconvolution Analysis
131 (SC_DCN_SPCTRL_ANL) Module Documentation, Version 13.18, SLB manual, Houston, TX, 2025c.

132 SLB: Omega Geophysical Processing System – F-X Coherent Noise Suppression (FXCNS) Module
133 Documentation, Version 3.16, SLB manual, Houston, TX, 2025d.

134 Yilmaz, Ö.: Seismic data analysis: Processing, Inversion, and Interpretation of Seismic Data, Appendix B.8
135 (Surface-Consistent Deconvolution), Society of Exploration Geophysicists, 262–266 pp., 2001.